polynomial in x and t, say $q(x, t)$, that satisfies the heat equation for all x and all t and for which $q(x, 0) = p(x)$.

(3.20) Prove that for $p(x) = x^n$ ($n = 0, 1, 2, 3, \ldots$) the polynomial

$$v_n(x, t) = n! \sum_{k=0}^{[n/2]} \frac{t^k}{k!} \frac{x^{n-2k}}{(n-2k)!}$$

is the unique polynomial discussed in (3.19). [The expression $[n/2]$ stands for the largest integer $\leq n/2$.] In particular, $v_0(x, t) = 1$, $v_1(x, t) = x$, $v_2(x, t) = x^2 + 2t$, $v_3(x, t) = x^3 + 6xt$.

(3.21) Define w_n as $n!$ times the nth coefficient in the power series expansion in z of e^{zx+z^2t}, that is, $e^{zx+z^2t} = \sum_{n=0}^{\infty} w_n(x, t)(z^n/n!)$. Prove that (a) w_n is a polynomial in x and t, (b) $w_n(x, 0) = x^n$, (c) w_n solves the heat equation, and (d) $w_n(x, t) = v_n(x, t)$ from (3.20).

Remark. The *heat polynomial* w_n described in (3.21) is closely related to the Hermite polynomial H_n discussed in the Miscellaneous Exercises for Chapter 6. Putting t equal to -1 and replacing x by $2x$ in the power series expansion given in (3.21), we obtain

(3.22)
$$e^{2xz-z^2} = \sum_{n=0}^{\infty} w_n(2x, -1)\frac{z^n}{n!}$$

and from (3.21d) we have

(3.23)
$$w_n(2x, -1) = n! \sum_{k=0}^{[n/2]} \frac{(-1)^k}{k!} \frac{(2x)^{n-2k}}{(n-2k)!}$$

The left side of (3.22) is the *generating function* for the Hermite polynomials, while the right side of (3.23) is the explicit expression for the nth Hermite polynomial $H_n(x)$. [See Davis (1975), p. 368.] Thus $H_n(x) = w_n(2x, -1)$.

Part B. Fourier Optics

§4. Fraunhofer Diffraction

Fraunhofer diffraction of light is fundamental in optics. It plays a key role in imaging with lenses, two important cases being telescopes and microscopes. Fraunhofer diffraction also occurs when a crystal diffracts an X-ray beam; this diffraction opens the way to identifying the underlying crystal structure. *In terms of Fourier analysis, Fraunhofer diffraction is a physical Fourier transform operation.*

Since this is not an optics text, we do not have sufficient space for a rigorous discussion of diffraction. Instead, we will only give an outline

[similar to the one given in Lipson and Lipson (1981), pp. 163–165] of how the Fourier transform comes into play. *In §§5–9, we shall see that this relationship is amply verified by the quantitative and qualitative description it gives of actual diffraction patterns.* The reader who desires a complete discussion of the underlying theory of diffraction should consult Goodman (1968), Iizuka (1985), or Lipson and Lipson (1981).

Suppose that a plane parallel wave of light, of wavelength λ, is cast upon an opaque screen in which there is a tiny aperture. Let a lens collect all the light emerging from the aperture and project it to its focal plane. As shown in Figure 7.1, the lens takes each bundle of parallel light rays and brings it to a focus.

Let the optic axis of the lens lie along the z axis and the aperture plane be the x–y plane located at $z = 0$. Suppose that $\mathcal{P}$ is a point in the aperture with coordinates $(x, y, 0)$. We will now argue that, because the wave front emerging from the point $\mathcal{P}$ has an amplitude $A(x, y)$, *the physical effect of the shuffling of light rays*, shown in Figure 1(*b*), *is to Fourier transform this amplitude function* $A(x, y)$. In Figure 7.2 we show light rays from $\mathcal{O}$ and $\mathcal{P}$, each parallel to the unit vector $\mathbf{u} = (\ell, m, n)$, coming to a focus $\mathcal{Q}$ after passing through points $\mathcal{O}_1$ and $\mathcal{P}_1$ in the lens. By Hamilton's version of Fermat's principle, light rays always lie normal to wave fronts of equal phase. Therefore, we shall imagine that the light ray from $\mathcal{P}$ has instead emanated from $\mathcal{P}_0$, the projection of $\mathcal{P}$ onto the plane normal to $\mathbf{u}$ and passing through $\mathcal{O}$ (as shown in Figure 7.2). Then the wave fronts along the rays $\mathcal{P}_0\mathcal{P}_1\mathcal{Q}$ and $\mathcal{O}\mathcal{O}_1\mathcal{Q}$ will arrive at $\mathcal{Q}$ in phase. Thus (because the wavelength is λ)

(4.1)
$$e^{i(2\pi/\lambda)|\mathcal{P}_0\mathcal{P}_1\mathcal{Q}|} = e^{i(2\pi/\lambda)|\mathcal{O}\mathcal{O}_1\mathcal{Q}|}$$

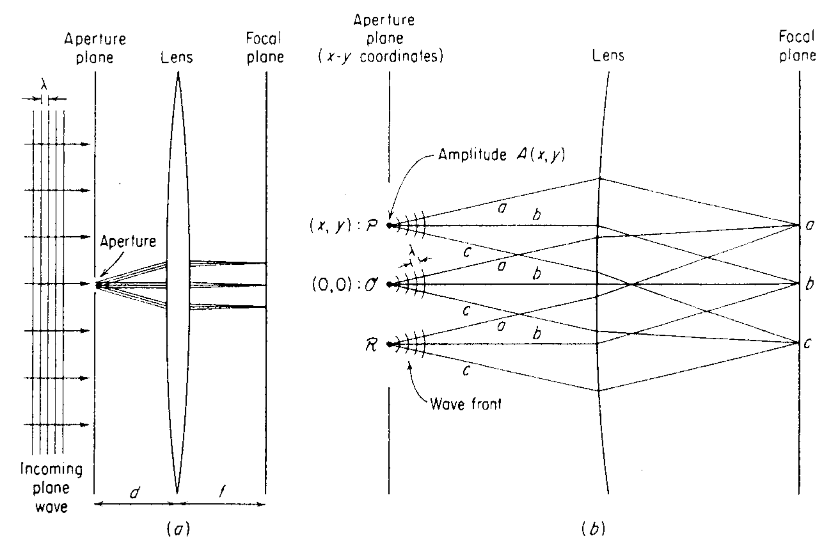

Figure 7.1 Focusing of bundles of parallel light rays by a lens. (*b*) An enlarged view of (*a*).

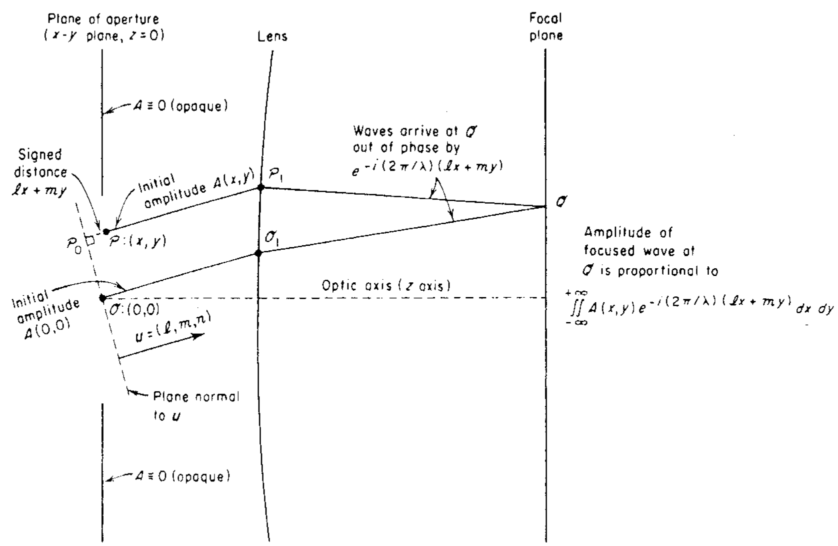

Figure 7.2 Focusing of two rays parallel to $\mathbf{u} = (\ell, m, n)$.

where $|\mathscr{P}_0\mathscr{P}_1\mathscr{Q}|$ and $|\mathscr{O}\mathscr{O}_1\mathscr{Q}|$ are the (optical) lengths of the two rays. Since $|\mathscr{P}_0\mathscr{P}_1| = \ell x + my$ we have the following phase relations

$$\textbf{(4.2)}\qquad \begin{aligned} e^{i(2\pi/\lambda)|\mathscr{P}_0\mathscr{P}_1\mathscr{Q}|} &= e^{i(2\pi/\lambda)|\mathscr{P}_0\mathscr{P}|}e^{i(2\pi/\lambda)|\mathscr{P}\mathscr{P}_1\mathscr{Q}|} \\ &= e^{i(2\pi/\lambda)(\ell x+my)}e^{i(2\pi/\lambda)|\mathscr{P}\mathscr{P}_1\mathscr{Q}|} \end{aligned}$$

Comparing (4.2) with (4.1) we obtain

$$\textbf{(4.3)}\qquad e^{i(2\pi/\lambda)|\mathscr{P}\mathscr{P}_1\mathscr{Q}|} = e^{i(2\pi/\lambda)|\mathscr{O}\mathscr{O}_1\mathscr{Q}|}e^{-i(2\pi/\lambda)(\ell x+my)}$$

Thus the wave fronts from $\mathscr{O}$ and $\mathscr{P}$ arrive at $\mathscr{Q}$ with amplitudes $A(0,0)\cdot e^{i(2\pi/\lambda)|\mathscr{O}\mathscr{O}_1\mathscr{Q}|}$ and $A(x,y)e^{i(2\pi/\lambda)|\mathscr{O}\mathscr{O}_1\mathscr{Q}|}e^{-i(2\pi/\lambda)(\ell x+my)}$, respectively. Therefore, the total amplitude Ψ at $\mathscr{Q}$ is given by the superposition integral

$$\textbf{(4.4)}\qquad \Psi = e^{i(2\pi/\lambda)|\mathscr{O}\mathscr{O}_1\mathscr{Q}|}\iint_{-\infty}^{+\infty} A(x,y)e^{-i(2\pi/\lambda)(\ell x+my)}\,dx\,dy$$

Since the screen is opaque outside the aperture, we may assume that $A(x,y)=0$ for (x,y) outside the aperture. Hence the integral in (4.4) is actually taken only over a finite region of the x–y plane.

Introducing the variables

$$\textbf{(4.5)}\qquad u = \ell/\lambda \qquad v = m/\lambda$$

we can write (4.4) in the form

$$\textbf{(4.6)}\qquad \Psi = e^{i(2\pi/\lambda)|\mathscr{O}\mathscr{O}_1\mathscr{Q}|}\hat{A}(u,v)$$

Experimentally, it is found that when the wave amplitude Ψ is recorded,

either photographically or by striking an observation screen, we record only the intensity $I = |\Psi|^2$. Hence, from (4.6) we have

$$\boxed{\textbf{(4.7)}\qquad I = |\Psi|^2 = |\hat{A}(u,v)|^2}$$

Because of (4.6) and (4.7) we say that the focal plane of the lens is *coincident* with the Fourier transform (u–v) plane. The variables u and v are called the *spatial frequencies* of the light amplitude emanent from the aperture.

If we introduce Cartesian coordinates X, Y into the focal plane (with origin on the optic axis), then we wish to know the relationship between those coordinates and the spatial frequencies. In the *paraxial approximation* $[(\ell, m, n) \approx (\ell, m, 1)]$ the relationship is approximately *linear*

$$\textbf{(4.8)}\qquad X \approx f\ell = (f\lambda)u \qquad Y \approx fm = (f\lambda)v$$

where f is the distance from the lens to the focal plane.[3] Thus, *the greater the wavelength λ the greater the $X-Y$ dimensions of the diffraction pattern formed by Ψ in the focal plane.*

In (4.6) there is a phase factor $e^{i(2\pi/\lambda)|\mathscr{O}\mathscr{O}_1\mathscr{Q}|}$ that depends upon the point $\mathscr{Q}$ in the focal plane. *This dependency can be removed by placing the aperture plane exactly f units from the lens.* In this case, a plane wave emanating in parallel from the focal plane (rays parallel to the optic axis) is focused by the lens onto the point $\mathscr{O}$. Conversely, all waves emanating from $\mathscr{O}$ arrive at the focal plane in phase (Fermat's principle). Thus $e^{i(2\pi/\lambda)|\mathscr{O}\mathscr{O}_1\mathscr{Q}|} = e^{i(2\pi/\lambda)2f}$ where $e^{i(2\pi/\lambda)2f}$ is the phase change along the ray from $\mathscr{O}$ to the focal plane that lies along the optic axis. Thus (4.6) becomes

$$\textbf{(4.9)}\qquad \Psi = e^{i4\pi f/\lambda}\hat{A}(u,v)$$

Formula (4.9) *shows that the light amplitude Ψ at the focal plane is*, except for a constant factor, *equal to the Fourier transform $\hat{A}$ of the amplitude function A of the light emanating from the aperture.*

The simplest form for the amplitude function A is

$$\textbf{(4.10)}\qquad A(x,y) = \begin{cases} 1 & \text{if } (x,y) \text{ is in the aperture} \\ 0 & \text{if } (x,y) \text{ is not in the aperture} \end{cases}$$

This function A corresponds to perfect transmission of the incoming plane wave (assumed to have constant amplitude 1 and phase e^{i0} when it strikes the aperture screen) through the aperture. We will call the function in (4.10) an *aperture function*. Other types of amplitude functions which correspond to partial absorption and/or partial phase variations introduced by apertures of varying material compositions.

3. Formula (4.8) is obtained by considering the *straight* ray $\mathscr{R}\mathscr{R}_1\mathscr{Q}$ parallel to $(\ell, m, 1)$ that passes through the point $\mathscr{R}_1$ on the lens that lies on the optic axis.

(4.11) Remark. Fraunhofer diffraction also occurs without a lens. This happens when X-rays are diffracted by crystals (or when a narrow laser beam shines through a small aperture to a screen on the other side of an optics lab). Roughly speaking, the analysis above will still apply if the light rays arriving at each point in the observation screen can be considered as approximately parallel. This is the case with both of the examples mentioned above (if only a small portion of the observation screen is viewed). For more details, see the references above, or Hecht and Zajec (1974).

Exercises

(4.12) Explain why light in the red spectrum is diffracted more than light in the blue spectrum. (How does this compare with refraction of light?) Why is white light split into a spectrum of colors by diffraction?

(4.13) Suppose that (4.8) applies throughout the focal plane. Show that the result of the lens system shown in Figure 7.3 is to produce an inverted and magnified (reduced) image of the aperture screen. The magnification (reduction) factor being $M = f_2/f_1$.

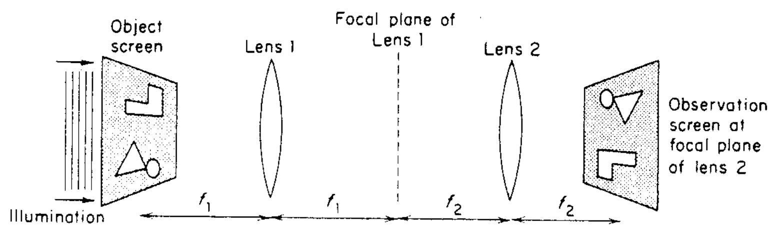

Figure 7.3 Double lens imaging system.

(4.14) In this section we assumed that the lens collects all the light from the aperture. A more realistic situation is depicted in Figure 7.4, where $P(u, v) = 0$ for sufficiently large values of u or v. Show that the result of

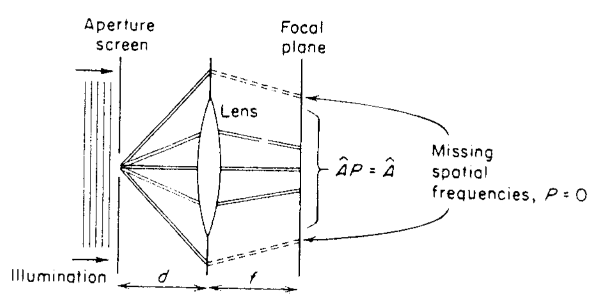

Figure 7.4 Diffraction limitation of lens. [Note that this figure requires that we observe only a portion of the focal plane near the optic axis to see the transform $|\hat{A}|^2$.]

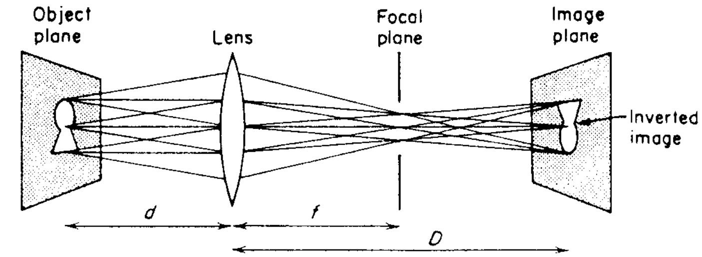

Figure 7.5 Imaging in geometrical optics. The lens equation $1/d + 1/D = 1/f$ holds.

(4.13) must be modified; the image of the aperture has the form $P_2[U_g * h_1]$ where h_1, P_2, and U_g are defined in an appropriate way.

(4.15) The classic imaging diagram of geometrical optics is shown in Figure 7.5. Interpret this figure in terms of Fourier analysis. How does the more realistic situation in Figure 7.4 affect what is depicted in Figure 7.5?

§5. Rectangular Apertures

The simplest apertures for Fourier analysis are the rectangular ones. Suppose we have a rectangular aperture of width $a > 0$ in the x direction and height $b > 0$ in the y direction, and the aperture is centered at the origin. [See Figure 7.8(a)]. If we let

$$A(x, y) = \begin{cases} 1 & \text{if } |x| < \tfrac{1}{2}a \quad \text{and} \quad |y| < \tfrac{1}{2}b \\ 0 & \text{otherwise} \end{cases}$$

then by Example (7.6c), Chapter 6, we have

$$\hat{A}(u, v) = \frac{\sin \pi a u}{\pi u} \frac{\sin \pi b v}{\pi v}$$

Therefore, the intensity $I = |\hat{A}|^2$ is given by

$$\textbf{(5.1)} \qquad I(u, v) = \frac{\sin^2 \pi a u}{(\pi u)^2} \frac{\sin^2 \pi b v}{(\pi v)^2} = a^2 b^2 \operatorname{sinc}^2 au \operatorname{sinc}^2 bv$$

The function I has the graph shown in Figure 7.6. Based on Figure 7.6 we can predict a diffraction pattern like the one shown in Figure 7.7. There are regions of brightness, marked off by fringes of zero intensity along the lines $u = \pm 1/a, \pm 2/a, \pm 3/a, \ldots$, and $v = \pm 1/b, \pm 2/b, \pm 3/b, \ldots$, that are the zeroes of $\operatorname{sinc}^2 au$ and $\operatorname{sinc}^2 bv$. The zone of highest brightness is a lozenge shaped region centered at the origin with u width $2/a$ and v height $2/b$. Notice the reciprocal relationship between the dimensions of the rectangular aperture and the dimensions of the central zone of brightness in the diffraction pattern, as well as the distances $\Delta u = 1/a$ and $\Delta v = 1/b$ between the fringes of zero intensity.

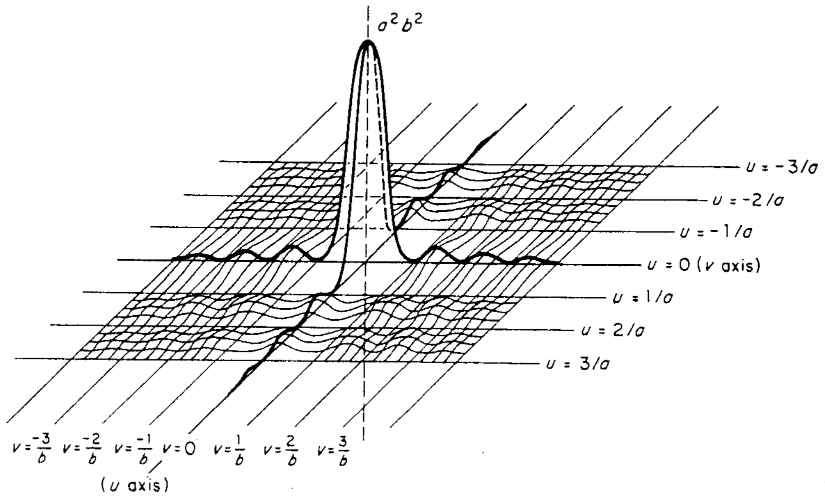

Figure 7.6 Graph of the intensity distribution I for a rectangular aperture. The graph is obtained by treating $1/(\pi u)^2[1/(\pi v)^2]$ as an envelope for $\sin^2 \pi au$ $[\sin^2 \pi bv]$ and noting that $\lim_{u\to 0} \sin^2 \pi au/(\pi u)^2 = a^2$ $[\lim_{v\to 0} \sin^2 \pi bv/(\pi v)^2 = b^2]$.

An actual diffraction pattern is shown in Figure 7.8(b). The reciprocal relationship between aperture detail and diffraction pattern detail, which we noted above, will be manifested in all of our examples. Diffraction patterns are often said to exist in *reciprocal space* (relative to apertures in real space).

If b is considerably larger than a then we obtain a *vertical slit.* Because the details of the pattern in Figure 7.7 *in the v direction* are proportional to $1/b$, for large b the pattern in Figure 7.7 will be squashed in the v direction. In Figure 7.9 we have a photograph of the diffraction pattern of a vertical slit.

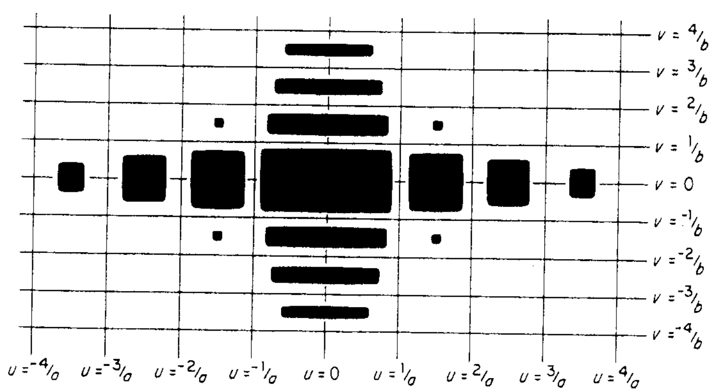

Figure 7.7 Predicted diffraction pattern (negative image) of a rectangular aperture.

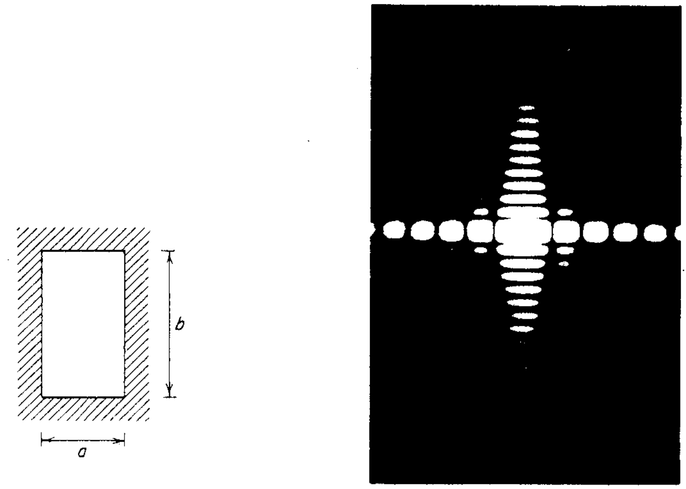

(a) (b)

Figure 7.8 (b) An actual diffraction pattern produced by a rectangular aperture similar to t one shown in (a). (Photograph courtesy of S. G. Lipson.)

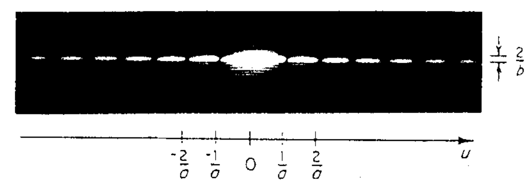

Figure 7.9 Diffraction pattern for a vertical slit. (Photograph courtesy of S. G. Lipson.)

Exercises

(5.2) Show that the maximum intensity of the diffraction pattern of rectangular aperture is proportional to the square of the area of th aperture.

(5.3) Suppose two identical rectangular apertures are separated by distance d along the x axis, as shown in Figure 7.10. Describe the diffractio pattern from such an aperture. What happens as d is increased?

(5.4) Suppose two identical rectangular apertures have their cente located at $(\frac{1}{2}c, -\frac{1}{2}d)$ and $(-\frac{1}{2}c, \frac{1}{2}d)$ as shown in Figure 7.11. Describe th diffraction pattern from such an aperture.

(5.5) Suppose the amplitude function A has the form shown in Figur 7.12. Describe the diffraction pattern from such an aperture and compare

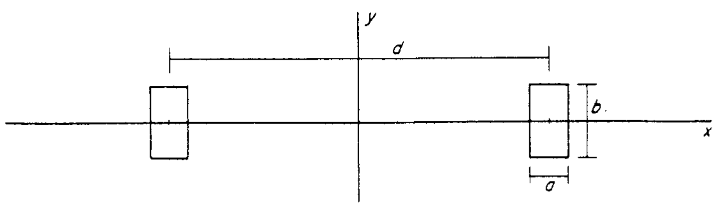

Figure 7.10 Aperture for Exercise (5.3).

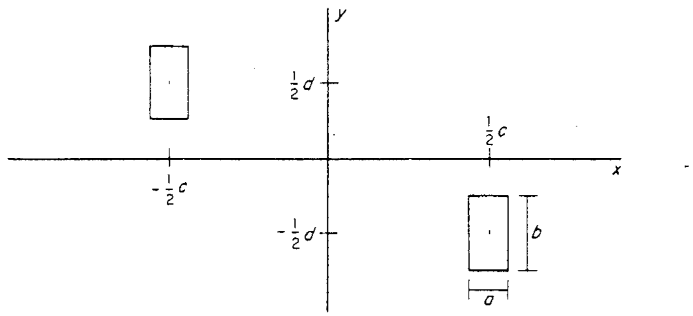

Figure 7.11 Aperture for Exercise (5.4).

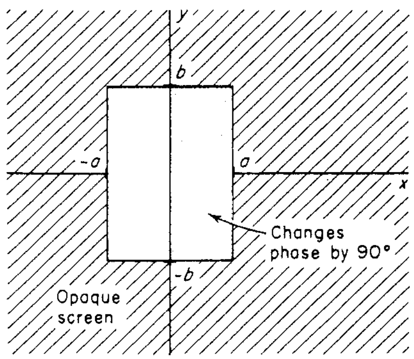

$$A(x,y)=\begin{cases}1, \text{ if } |y|<b,\ -a<x<0\\ e^{i\pi/2}, \text{ if } |y|<b,\ 0<x<a\\ 0, \text{ otherwise}\end{cases}$$

Figure 7.12 Aperture and aperture function for Exercise (5.5).

with Figure 7.8(b). **Remark.** Such an aperture can be made by placing a sheet of mica over half of a simple rectangular aperture; the mica induces a 90° phase shift of the incoming light wave.

§6. Circular Apertures

Consider a circular aperture of radius a. The aperture function in this case is a radial function (§7, Chapter 6)

$$A(r)=\begin{cases}1 & \text{if } 0\le r<a\\ 0 & \text{if } r>a\end{cases}$$

where $r=(x^2+y^2)^{1/2}$. Using Theorem (7.15), Chapter 6, we have

$$\textbf{(6.1)}\qquad \hat{A}(\rho)=2\pi\int_0^a J_0(2\pi\rho r)r\,dr$$

where $\rho=(u^2+v^2)^{1/2}$. If we let $s=2\pi\rho r$, then

$$\textbf{(6.2)}\qquad \hat{A}(\rho)=\frac{1}{2\pi\rho^2}\int_0^{2\pi\rho a} sJ_0(s)\,ds$$

Let's consider the function $H(x)=\int_0^x sJ_0(s)\,ds$ for $x\ge 0$. We have

$$\textbf{(6.3)}\qquad dH/dx=xJ_0(x)\qquad (x\ge 0)$$

But, by a recurrence relation for Bessel functions [(2.1b), Chapter 10] we have

$$\textbf{(6.3')}\qquad (d/dx)[xJ_1(x)]=xJ_0(x)\qquad (x\ge 0)$$

where [see (2.2), Chapter 10]

$$J_1(x)=\frac{1}{2\pi}\int_{-\pi}^{\pi} e^{ix\sin\phi}e^{-i\phi}\,d\phi$$

Noting that J_1 is continuous at $x=0$, and has the value 0 there, we conclude from (6.3) and (6.3′) that $H(x)=xJ_1(x)$ for $x\ge 0$. Therefore, we can rewrite (6.2) as

$$\textbf{(6.4)}\qquad \hat{A}(\rho)=\frac{a}{\rho}J_1(2\pi\rho a)=\pi a^2\left[\frac{2J_1(2\pi\rho a)}{2\pi\rho a}\right]$$

Therefore, the intensity I is given by

$$\textbf{(6.5)}\qquad I(\rho)=(\pi a^2)^2\left[\frac{2J_1(2\pi\rho a)}{2\pi\rho a}\right]^2\qquad [\rho=(u^2+v^2)^{1/2}]$$

The function J_1 has been extensively tabulated[4] and so the graph of I is well known. (See Figure 7.13.) The graph of I can also be sketched using asymptotic formulas for J_1 that we shall discuss in Chapter 10.

Figure 7.13(b) gives a nice prediction for the diffraction pattern, as we can see from Figure 7.14. The rings in the pattern are called *Airy's rings* and the whole pattern is called *Airy's pattern.*

Notice that the radius of the central disk, bounded by the zero intensity (dark) ring at $\rho \doteq 3.83/2\pi a$, grows larger with decreasing radius a. Furthermore, as this radius decreases the location of Airy's rings (bright and dark) increases away from the origin. These results illustrate again the reciprocal relationship between aperture detail and diffraction pattern (transform) detail.

Airy's rings are observed when a telescope with too small an aperture attempts to resolve the image of a distant star. *The resulting image is the*

4. See Watson (1944), pp. 667–697.

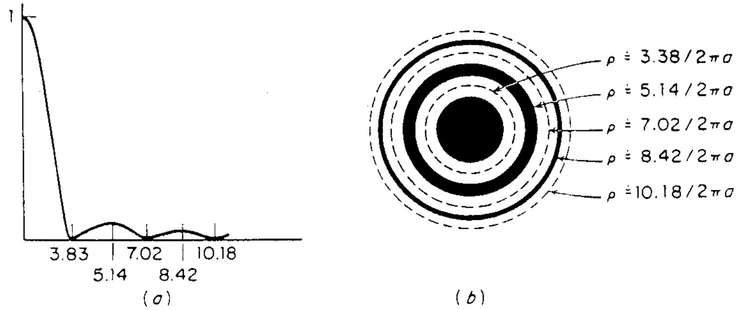

Figure 7.13 Diffraction from a circular aperture. (*a*) Graph of $[2J_1(x)/x]^2$. (*b*) Prediction for the diffraction pattern.

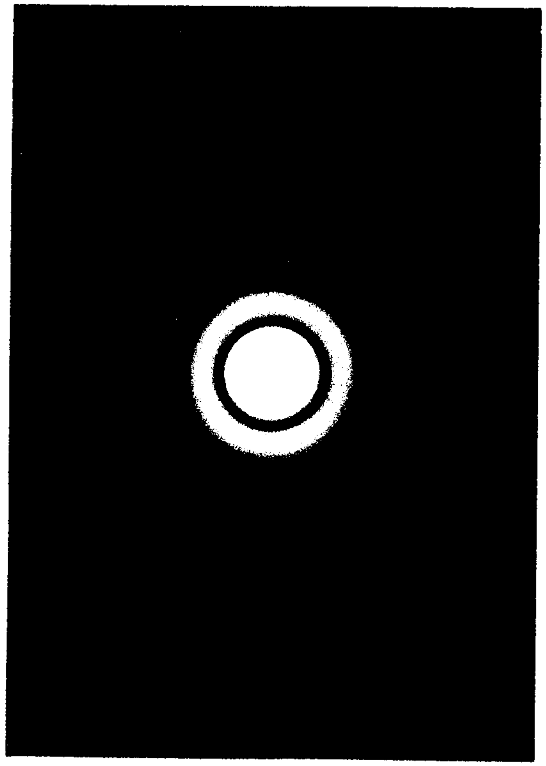

Figure 7.14 Diffraction pattern from a circular aperture. (Photograph courtesy of S. G. Lipson.)

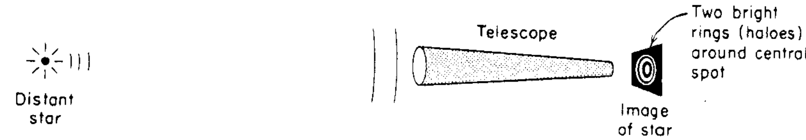

Figure 7.15 Airy pattern observed in telescopes.

diffraction pattern of the aperture. (See Figure 7.15.) The astronomer Airy first predicted this ring pattern. Because of the large wavelengths used, this diffraction is a serious problem encountered with radio telescopes (where the aperture is the collecting dish).

Exercises

(6.6) Show that the intensity of Airy's pattern increases with the square of the area of the circular aperture, and that the position of Airy's rings increases inversely to the circumference of the circular aperture.

(6.7) Explain why a circular aperture with a small enough radius will have a Fraunhofer diffraction pattern consisting only of a disk. [*Hint:* See (4.11) and Figure 7.4.] Such an aperture is called a *pinhole*.

(6.8) How would the Airy patterns differ between light of wavelength $\lambda_1 = 750 \times 10^{-9}$ m (red light) versus light of $\lambda_2 = 500 \times 10^{-9}$ m (bluish green light)? Describe the effect of shining white light through circular apertures of various radii. (This phenomenon occurs in color movies occasionally.)

(6.9) Let the aperture consist of an annular ring with aperture function

$$A(x, y) = \begin{cases} 1 & \text{if } a < (x^2 + y^2)^{1/2} < b \\ 0 & \text{otherwise} \end{cases}$$

Describe the resulting diffraction patterns for $a \ll b$ and for a close to b.

(6.10) *Babinet's Principle.* One aperture is called *complementary* to a second aperture if their aperture functions A_1, A_2 satisfy $A_1 + A_2 = A_0$ where A_0 is a large circular (or rectangular) aperture function. Show that *the two complementary apertures have identical diffraction patterns*, except for a small region about the origin in the u–v plane.

§7. Interference

The study of interference is an important area of application of Fourier analysis in optics. In this section we will treat some simple examples of interference. The more important cases of diffraction gratings and the array theorem will be discussed in the next two sections.

Suppose that two circular apertures of radius a are centered at $x = \pm\frac{1}{2}d$ on the x axis. In this case our aperture function will be (assuming $d > 2a$)

$$A(x, y) = A_1(x + \tfrac{1}{2}d, y) + A_1(x - \tfrac{1}{2}d, y)$$

where A_1 is the aperture function for a circular aperture that we considered in the previous section. Using the shift property and linearity we obtain

$$\hat{A}(u, v) = \hat{A}_1(u, v)[e^{i\pi du} + e^{-i\pi du}] = 2\cos \pi du \hat{A}_1(u, v)$$

hence for the intensity I we have

(7.1) $$I(u, v) = 4\cos^2 \pi du\, |\hat{A}_1(u, v)|^2 = 4\cos^2 \pi du\, I_1(u, v)$$

where I_1 is the intensity for a single circular aperture.

Since $4\cos^2 \pi du$ equals 0 when $u = \pm 1/(2d), \pm 3/(2d), \pm 5/(2d), \ldots$, we expect zero intensity along vertical lines in the u–v plane defined by those u values. In view of (7.1) we expect dark vertical strips, *interference fringes*, to overlap the Airy pattern shown in Figure 7.14. (Also, we expect amplification along the lines $u = 0, \pm 1/d, \pm 2/d, \ldots$, where $4\cos^2 \pi du$ has its maximum value of 4.) In Figure 7.16 we show the diffraction pattern from two such circular apertures.

For a second example, consider two identical rectangular apertures positioned as indicated in Figure 7.11. The aperture function in this case is

$$A(x, y) = A_1(x - \tfrac{1}{2}c, y + \tfrac{1}{2}d) + A_1(x + \tfrac{1}{2}c, y - \tfrac{1}{2}d)$$

which was considered in Example (7.6d), Chapter 6. Using the transform found in that example, we obtain

$$I(u, v) = 4\cos^2 \pi(cu - dv) I_1(u, v)$$

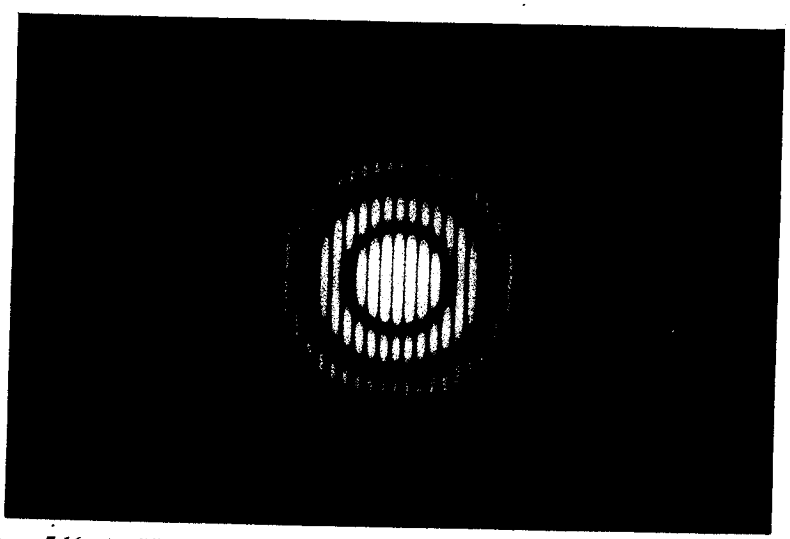

Figure 7.16 A diffraction pattern from two horizontally separated circular apertures. (Photograph courtesy of S. G. Lipson.)

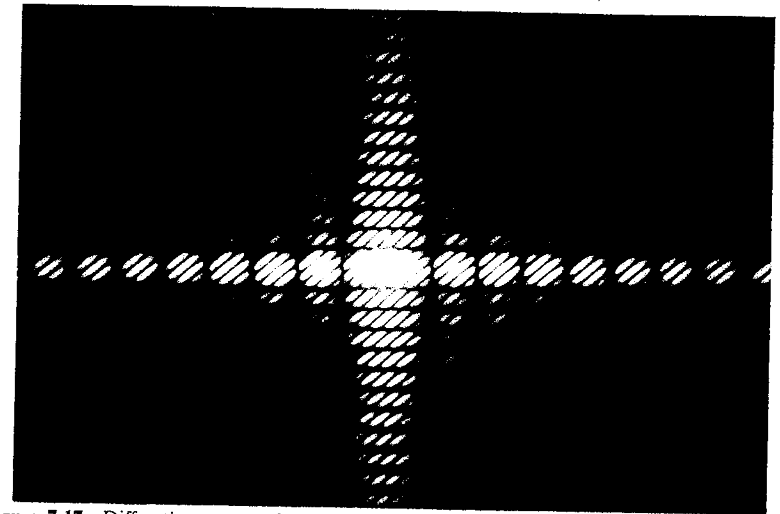

Figure 7.17 Diffraction pattern from two rectangular apertures (here $c/d = 1$). (Photograph courtesy of S. G. Lipson.)

where I_1 is the intensity distribution for a single rectangular aperture. The interference fringes lie along lines given by $cu - dv = \tfrac{1}{2}k$ for $k = \pm 1, \pm 3, \pm 5, \ldots$. Those dark fringes lie over the diffraction pattern for a single rectangular aperture at parallel directions with slope c/d, hence perpendicular to the line segment that connects the centers of the two apertures. Figure 7.17 shows the actual diffraction pattern that results in this case.

Exercises

(7.2) Show that interference fringes always occur when an aperture consists of two identical apertures.

(7.3) Show that the number of interference fringes per unit length in both the examples for this section is proportional to the distance between the centers of the apertures.

(7.4) Describe the diffraction pattern of three equally spaced similar vertical slits. [*Hint*: Add the transform of the center slit to that of the two outer ones.] Now do four equally spaced vertical slits.

(7.5) Suppose we have four pinholes [see Exercise (6.7)] arranged in a parallelogram, that is, the pinholes are placed at (d_1, d_2), $(c_1, -c_2)$, $(-d_1, -d_2)$, and $(-c_1, c_2)$ where c_1, c_2, d_1, and d_2 are positive. Describe the resulting diffraction pattern.

§8. Diffraction Gratings

Diffraction gratings were first constructed by Fraunhofer in the 1830's. They are an essential tool of modern science.

Suppose that an aperture consists of a large number, say N, of vertical slits spaced equally far apart and very close together. Such an aperture is called a *diffraction grating*. Diffraction gratings with 100,000 slits have been constructed. If we assume that the first slit on the left side of the grating is centered at the origin, then $A(x, y) = \sum_{n=0}^{N-1} A_1(x - nd, y)$ where A_1 is the aperture function for a single vertical slit (see the end of §5), and d is the distance between the central axes of the slits. By the shifting and linearity properties we have

$$\hat{A}(u, v) = \sum_{n=0}^{N-1} \hat{A}_1(u, v)e^{-i2\pi n\, du} = \hat{A}_1(u, v)\sum_{n=0}^{N-1} [e^{-i2\pi\, du}]^n$$

$$= \hat{A}_1(u, v)\frac{1 - e^{-i2\pi N\, du}}{1 - e^{-i2\pi\, du}}$$

where we summed a finite geometric series to obtain the last quantity above. Factoring out $e^{-i\pi N\, du}/e^{-i\pi\, du}$ from the last fraction above we get

$$\hat{A}(u, v) = \hat{A}_1(u, v)\frac{e^{-i\pi N\, du}}{e^{-i\pi\, du}}\frac{\sin N\pi\, du}{\sin \pi\, du}$$

Hence, the intensity distribution I is given by

(8.1) $$I = I_1 \frac{\sin^2 N\pi\, du}{\sin^2 \pi\, du} = I_1 S$$

where I_1 is the intensity for a single vertical slit. In Figure 7.18 we have graphed the function S, called the *structure factor* for the grating, and its intensity distribution in the u–v plane. [Note: $S(u) = N \cdot F_N(2\pi\, du)$ where F_N is *Fejér's kernel.*] As an intensity distribution in the u–v plane, S is a sequence of vertical strips centered along the vertical lines $u = 0, \pm 1/d, \pm 2/d, \ldots$, each strip having a width no greater than $2/Nd$ and intensity N^2 along their central lines. When this sequence of strips is multiplied by I_1 (see Figure 7.9) it acts as a mask of *amplifiers* of power N^2 and we obtain a sequence of bright dots centered at $u = 0, \pm 1/d, \pm 2/d, \ldots$. (See Figure 7.19.) In Figure 7.20 we have an actual diffraction pattern resulting from a grating with a small number of lines ($N = 55$). As the reader can see, *away from the central vertical axis*, the prediction of a sequence of bright dots is confirmed in Figure 7.20. The slight discrepancy between Figures 7.19 and 7.20 along that central vertical axis is easily explained [see Exercise (8.4)].

Diffraction gratings are primarily used for the production of spectra. If we shine white light through the diffraction grating considered above, then because of formula (4.5) we will obtain a *spectral decomposition* of that light. From Figure 7.19, we see that the spacing between dots is $\Delta u = 1/d$ hence from (4.5) we have[5]

(8.2) $$\Delta\ell = \lambda\, \Delta u = \lambda/d$$

5. We are assuming here that white light is a linear superposition of all its wavelengths and that passing the light through the grating is a linear process, assumptions that are confirmed in practice.

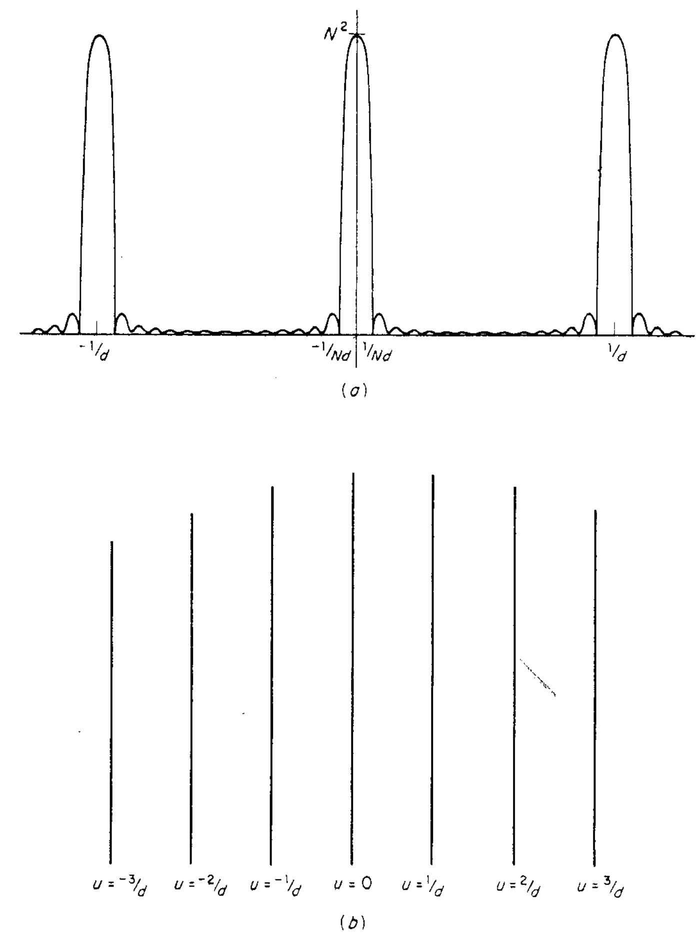

Figure 7.18 (a) The graph of $S(u) = \sin^2 N\pi\, du/\sin^2 \pi\, du$ is shown. (b) We have graphed the intensity distribution in the u–v plane that is generated by $S(u)$, *ignoring secondary peaks.*

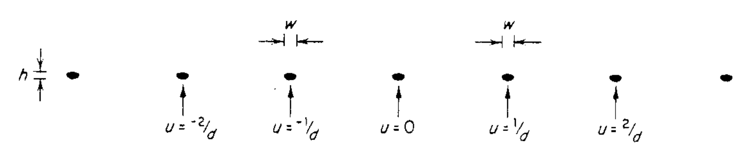

Figure 7.19 The intensity distribution resulting from a diffraction grating (negative image). The width w of each dot is no more than $2/Nd$, their height h is no more than $2/b$ where b is the height in the y direction of each vertical slit in the grating.

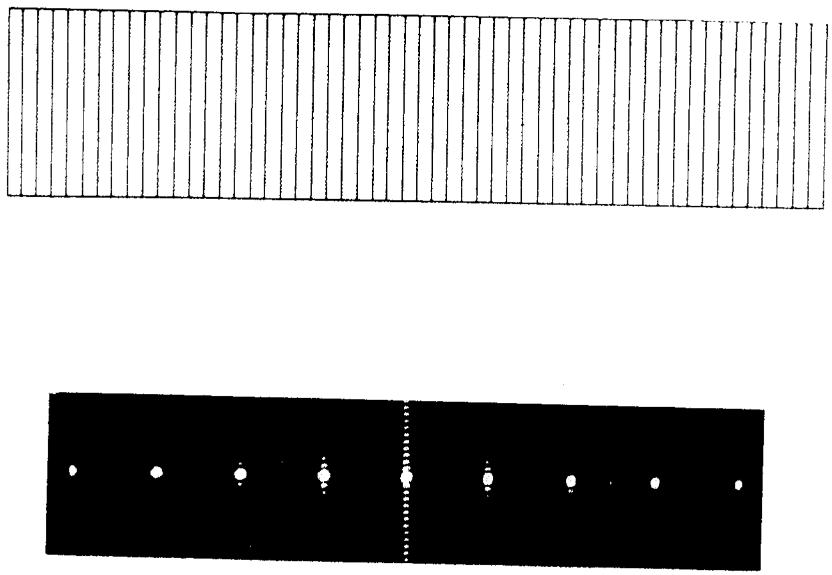

Figure 7.20 A grating of 55 narrow lines (the negative of the drawing on top), and its diffraction pattern (the photograph on the bottom). [Reproduced with permission from Lipson (1972), p. 358.]

is the *angular spacing* between the dots. Here we may take $\ell = \sin\theta$ where θ is the angle of diffracted rays to the optic axis (since $m \doteq 0$ because we have vertical slits). Comparing (8.2) with the ratios of the wavelengths of visible light in Table 7.1, we see that (8.2) describes a spreading out (dispersion) of white light into its spectrum of colors. (See Figure 7.21.) From Table 7.1 and Figure 7.21 we can see that the second-order spectrum is longer (greater dispersion) than the first-order spectrum. The third-order spectrum, which begins at $3\lambda_{red}/2d$ and ends at $3\lambda_{red}/d$, actually overlaps half of the second-order spectrum, which begins at λ_{red}/d and ends at $2\lambda_{red}/d$. The third-order spectrum is even more dispersed than the first two spectra.

Table 7.1 Approximate Wavelengths λ for the Visible Spectrum and Their Ratios to $\lambda_{red} = 780 \times 10^{-9}$ m

Color	λ (1×10^{-9} m)	λ/λ_{red}
Red	780–622	1.–0.797
Orange	622–597	0.797–0.765
Yellow	597–577	0.765–0.739
Green	577–492	0.739–0.631
Blue	492–455	0.631–0.583
Violet	455–390	0.583–0.5

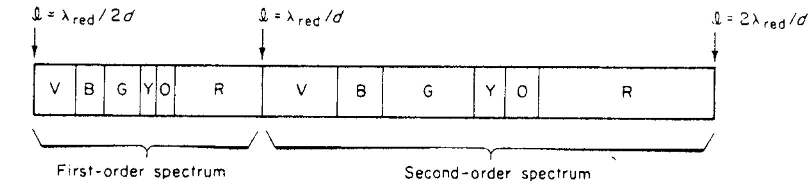

Figure 7.21 Spectra of white light from a diffraction grating.

Since each dot in Figure 7.19 has a width w, no greater than $2/Nd$, there will be a smearing of the colors in the spectra obtained by diffraction gratings. However, if Nd is very large, then $2/Nd$ will be very small and there will be less smearing (better *resolution*). In any case, the resolution is inversely proportional to Nd, the *length of the grating*. [See Exercise (8.7).]

We assumed above that white light was shined through the grating. The grating can be used, of course, to disperse the spectra of other kinds of light. By passing white light through a gas and then observing that light through a diffraction grating, we obtain spectra characterized by dark fringes (absorption lines) in the normal spectrum of white light. Depending on the element(s) composing the gas, certain characteristic absorption lines appear. Gas absorption spectroscopy is of some use in chemistry. Moreover, by observing the spectra of starlight, the composition of stars can be analyzed. The classic example is the discovery of helium in the sun. The absorption lines in solar light are sometimes called *Fraunhofer lines*. Another application is the analysis of the spectra of the light emitted from chemical reactions (emission spectra). For all of these applications, the problem of resolution of spectra is a vital one. [See Bell (1972).]

Exercises

(8.3) Sketch the graph of $y = I_1 S$ as a function of u when $v = 0$.

(8.4) Explain why there is a vertical strip of dots in the center of the diffraction pattern in Figure 7.20. Show that if Nd is large enough, then the dots in Figure 7.19 will actually be thin lines.

(8.5) Show that if the distance d between the vertical slits in a diffraction grating is equal to $2a$ (twice the width of each slit) then the second-order spectrum will be eliminated. Show also that the first-order spectrum is not overlapped by any of the higher order spectra. What value should d have so that the third (nth)-order spectra is eliminated?

(8.6) Let $d \doteq 8a$ and let h_0, h_1, h_2, h_3 stand for the first four highest maxima of the intensity function $I = I_1 S$. Show that

$$h_0 \doteq N^2a^2b^2 \qquad h_1 \doteq 0.95N^2a^2b^2 \qquad h_2 \doteq 0.81N^2a^2b^2 \qquad h_3 \doteq 0.62N^2a^2b^2$$

(8.7) Suppose that light containing two wavelengths $\lambda_1 < \lambda_2$ is transmitted through a diffraction grating. If λ_1 and λ_2 are close together, then their

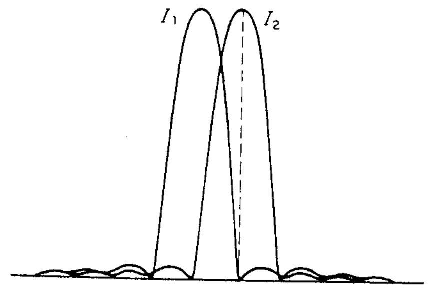

Figure 7.22 A central peak for I_2 lying over a first zero for I_1. This is known as *Rayleigh's criterion* for the resolution of two spectral lines.

spectral lines [see (8.4)] might smear together. How large does N have to be in order for a central peak (highest maxima) of I_2, the intensity function for λ_2, to lie over a first zero for I_1, the intensity function for λ_1? [See Figure 7.22] *Note*: your answer should depend on which spectrum (first, second, third, etc.) for λ_1 and λ_2 is being looked at.

(8.8) Show that resolution by Rayleigh's criterion [see problem (8.7)] is easier to obtain the higher the order of the spectrum.

(8.9) In spectroscopy, the second-order spectrum is usually preferred among all the orders. Can you think of any reasons for this?

§9. The Array Theorem

We now turn to a beautiful result in optics known as the *Array Theorem*. Let c and d be positive constants. Suppose that we have a collection of $M \cdot N$ identical apertures positioned in a rectangular array at points (mc, nd) for $m = 0, 1, \ldots, M-1$ and $n = 0, 1, \ldots, N-1$. (See Figure 7.23.) We assume that c and d are large enough so that none of the apertures overlaps.

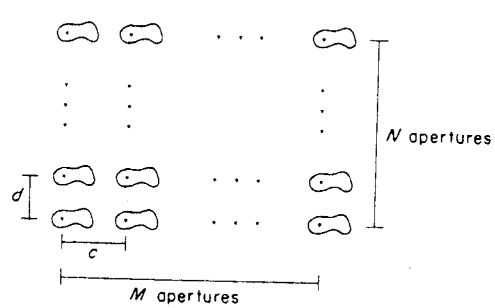

Figure 7.23 A rectangular array of identical apertures.

Letting A_1 denote the aperture function for a single aperture, and supposing that the origin in the x–y plane is located in the aperture at the lower left hand corner of the array, we have

$$A(x, y) = \sum_{m,n=0}^{M-1,N-1} A_1(x - mc, y - nd)$$

is the aperture function for the whole array. By linearity and shifting, we get

$$\hat{A}(u, v) = \sum_{m,n=0}^{M-1,N-1} \hat{A}_1(u, v)e^{-i2\pi(mcu+n\,dv)}$$

$$= \hat{A}_1(u, v)\left[\sum_{m=0}^{M-1} e^{-i2\pi mcu}\right]\left[\sum_{n=0}^{N-1} e^{-i2\pi n\,dv}\right]$$

From the result of the discussion of diffraction gratings in the previous section, we obtain

(9.1) $$I(u, v) = I_1(u, v)\frac{\sin^2 M\pi cu}{\sin^2 \pi cu}\frac{\sin^2 N\pi\,dv}{\sin^2 \pi\,dv}$$

Thus the intensity distribution I for the whole array is the product of the intensity distribution I_1 for a single aperture with the function S defined by

$$S(u, v) = \frac{\sin^2 M\pi cu}{\sin^2 \pi cu}\frac{\sin^2 N\pi\,dv}{\sin^2 \pi\,dv}$$

The function I_1 is called the *form factor* and the function S is called the *structure factor*.

We see that S is the product of the type of function treated in the previous section. The factor $\sin^2 N\pi\,dv/\sin^2 \pi\,dv$ has an intensity distribution consisting of horizontal strips lying along the lines $v = 0$, $\pm 1/d$, $\pm 2/d, \ldots$, and having intensity N^2. Hence, noting the results of the last section (especially Figure 7.18), we conclude that the structure factor S has an intensity distribution in the u–v plane consisting of a *rectangular array of dots* of intensity M^2N^2 centered at the intersections of vertical lines at $u = 0$, $\pm 1/c$, $\pm 2/c, \ldots$ and horizontal lines at $v = 0$, $\pm 1/d$, $\pm 2/d, \ldots$. These dots have $u - v$ dimensions no larger than $(2/Mc) \times (2/Nd)$. Between these dots are spaces of essentially zero intensity (if we ignore secondary maxima in S).

Thus the intensity distribution I in (9.1) is obtained by overlaying the intensity distribution for a single aperture by an array of dot amplifiers of internsity M^2N^2 located at the points $(m/c, n/d)$ for integers m and n. The larger the values of c and d the closer the dot amplifiers. The array of amplifiers is called the *reciprocal lattice* to the array of apertures.

(9.2) Example. Suppose that a square array of 11×11 circular apertures each having radius 0.5 mm is formed by setting $c = d = 3$ mm. The amplification of each dot amplifier will be 11^4. These dots will be positioned on a square array with $\Delta u = \Delta v = 0.333\ldots$. An Airy pattern for one circular

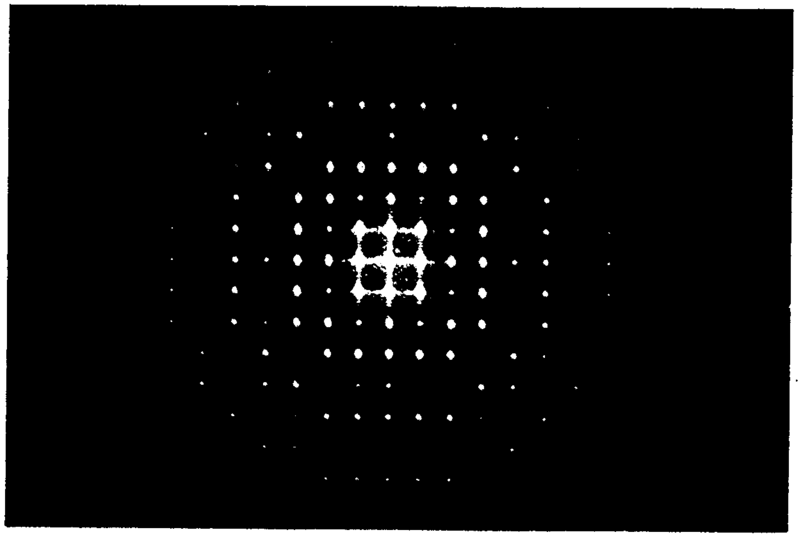

Figure 7.24 Diffraction pattern of 11 × 11 circular apertures. We have a grainy Airy pattern. The fine structure between the 9 dots nearest the center is due to secondary maxima in the structure factor. (Photograph courtesy of S. G. Lipson.)

aperture is overlayed by this square array of dot amplifiers. (See Figure 7.24.)

One important application of the array theorem is in radio astronomy. A large dish aerial will bring a radio wave to focus on its receiving device; thus, such an aperture acts like a *diffracting circular aperture*. By setting up an array of such dish aerials, the amplification of the array theorem can be brought into play. According to S. Lipson [see p. 384 of Lipson (1972)], "the sensitivity of such an array is almost as good as a filled aerial of the same dimensions." In other words, *by building a large array of dish aerials we can achieve the equivalent of a gigantic dish aerial covering the area of the array* (and the resolution improves when the dishes in the array are farther apart). [See Lipson and Lipson (1981), §11.6.]

The array theorem has also been applied in the study of protein molecules. The Fourier transform of an electron photomicrograph of a protein might contain high intensity dots lying along a (reciprocal) lattice, a sure sign that there is an *underlying periodic structure in the original micrograph* (that might not be evident due to random interference, called *noise*). For an excellent nontechnical discussion, see Unwin and Henderson (1984). See also Lipson (1972), pp. 401–413.

Exercises

(9.3) Describe the diffraction pattern of an array of 15×15 square apertures of dimensions $0.1\ \mathrm{mm} \times 0.1\ \mathrm{mm}$ formed by letting $c = d = 0.2\ \mathrm{mm}$.

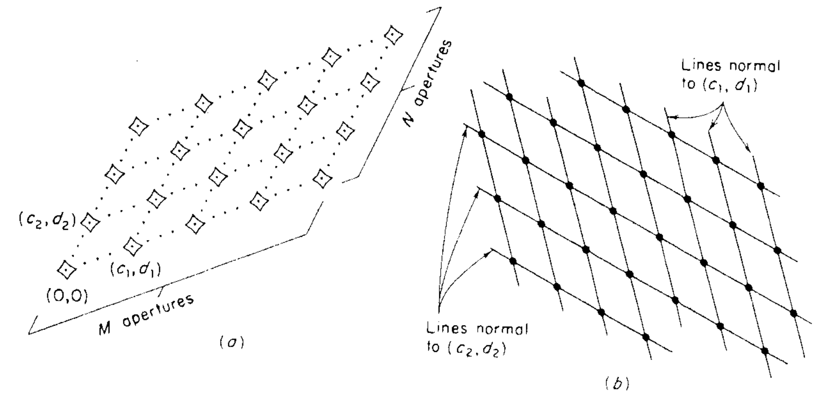

Figure 7.25 A parallelogram array of apertures and the intensity pattern for the structure factor. (*a*) Parallelogram array. (*b*) Reciprocal lattice.

(9.4) Show that the fine structure about the 9 central dots in Figure 7.24 consists of tiny diffraction patterns resembling those for a square aperture of $x - y$ dimensions $33 \times 33\ \mathrm{mm}^2$. [*Hint*: Compare the intensity patterns for $S(u, v)$ and the function $I(u, v)$ in Figure 7.6.] *Can you show the same result by applying the convolution theorem? *Note*: Beautiful pictures illustrating these ideas can be found in plate 13 of Harburn, Taylor, and Welberry (1975).

***(9.5)** *Parallelogram Array.* Suppose that $M \cdot N$ identical apertures are placed in a parallelogram array as shown in Figure 7.25(*a*). Show that the intensity distribution I for the diffraction pattern is equal to $I_1 S$ where I_1 is the intensity distribution for a single aperture and S is a structure factor. Show that S consists of an array of dot amplifiers, of intensity M^2N^2, situated at points of intersection of lines in a parallelogram configuration, where those lines are perpendicular to those of the array of apertures. [See Figure 7.25(*b*).] Describe the total diffraction pattern resulting from $I = I_1 S$. [*Hint*: Proceed as in the rectangular array case, but at an appropriate point substitute $\theta = c_1 u + d_1 v$ and $\phi = c_2 u + d_2 v$.]

Remark. The array of dots in Figure 7.25(*b*) is called the *reciprocal lattice* for the array of apertures.

(9.6) Same problem as (9.3), but the square apertures are situated on a parallelogram array formed by $\mathbf{v}_1 = (0.4\ \mathrm{mm},\ 0.4\ \mathrm{mm})$ and $\mathbf{v}_2 = (0.1\ \mathrm{mm},\ 0.2\ \mathrm{mm})$.

§10. Imaging Theory

In this section we shall briefly describe the theory of lens imaging via Fourier analysis. This theory is due to Abbe and Zernike.

In §4 we showed that the amplitude Ψ at each point $\mathscr{Q}$ in the focal plane of a lens is given by [see (4.6)]

$$\Psi(u, v) = e^{i(2\pi/\lambda)|\mathscr{O}\mathscr{O}_1\mathscr{Q}|}\hat{A}(u, v) \tag{10.1}$$

provided the object (aperture) is illuminated by monochromatic coherent light (i.e., a plane parallel wave with wavelength λ). This type of illumination is very common in science, due to the invention of the laser; it is also approximately fulfilled in microscopy (the illumination of the slide of a microscope is approximately coherent).

To see how an image is formed by a lens we must allow the rays, that have converged at the focal plane in Figure 7.1, to diverge and proceed to a further plane as shown in Figure 7.26. If we reason as in §4, then we can calculate the amplitude $\varphi(x, y)$ at a point $\mathscr{R}_2$ with coordinates $(x, y, d + D)$ in the image plane. We find that

$$\varphi(x, y) = \iint_{-\infty}^{+\infty} \Psi(u, v)e^{i(2\pi/\lambda)|\mathscr{Q}\mathscr{R}_2|}\, du\, dv \tag{10.2}$$

Hence we must determine the (optical) distance $|\mathscr{Q}\mathscr{R}_2|$ of each ray $\mathscr{Q}\mathscr{R}_2$. By the law of cosines (see Figure 7.27)

$$\begin{aligned} |\mathscr{Q}\mathscr{R}_2| &= [|\mathscr{Q}\mathscr{O}_2|^2 + (x^2 + y^2) - 2(x^2 + y^2)^{1/2}|\mathscr{Q}\mathscr{O}_2| \cos \tilde{\gamma}]^{1/2} \\ &\approx |\mathscr{Q}\mathscr{O}_2| - (x^2 + y^2)^{1/2} \cos \tilde{\gamma} \end{aligned} \tag{10.3}$$

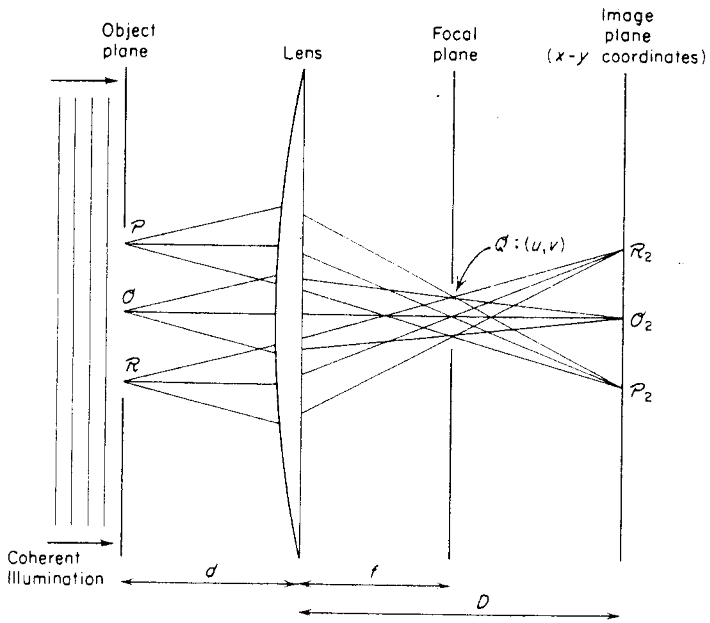

Figure 7.26 Each point in the focal plane emanates a wave, with amplitude Ψ. These waves converge at points in the image plane, a second Fourier transform operation.

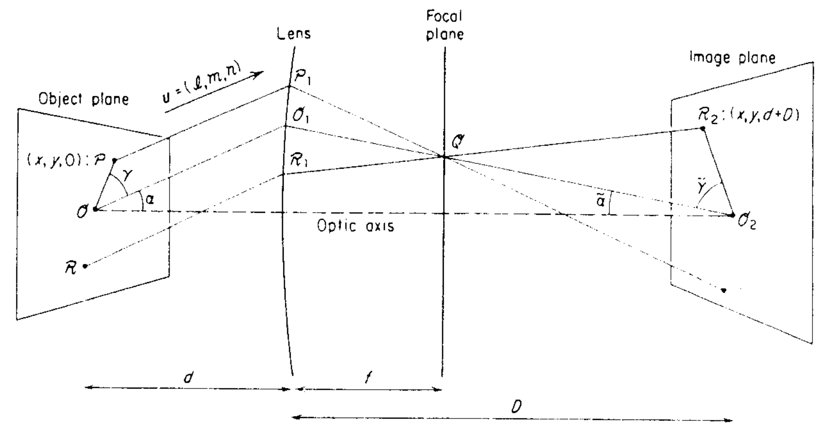

Figure 7.27 Ray diagram for the image–object derivation.

To justify the approximation in (10.3) we must assume that $(x^2 + y^2)^{1/2} \ll |\mathscr{Q}\mathscr{O}_2|$ *which will be the case if the image is assumed to be a small one.*

Letting $\tilde{\alpha}$ be the complementary angle (to $\tilde{\gamma}$) that $\mathscr{Q}\mathscr{O}_2$ makes with the z axis (optic axis) we can rewrite (10.3) as

$$|\mathscr{Q}\mathscr{R}_2| = |\mathscr{Q}\mathscr{O}_2| - (x^2 + y^2)^{1/2} \sin \tilde{\alpha} \tag{10.4}$$

We now invoke the *Abbe sine condition* which states the angles α and $\tilde{\alpha}$ should satisfy

$$\sin \alpha = M \sin \tilde{\alpha} \qquad \text{(Abbe sine condition)} \tag{10.5}$$

where M is a positive constant. Using (10.5), formula (10.4) becomes

$$\begin{aligned} |\mathscr{Q}\mathscr{R}_2| &= |\mathscr{Q}\mathscr{O}_2| - \frac{(x^2 + y^2)^{1/2} \sin \alpha}{M} \\ &= |\mathscr{Q}\mathscr{O}_2| - \frac{(x^2 + y^2)^{1/2}(\ell^2 + m^2 + n^2)^{1/2} \cos \gamma}{M} \end{aligned} \tag{10.6}$$

Here γ is the complementary angle (to α) that $\mathscr{O}\mathscr{O}_1$ makes with $\mathscr{O}\mathscr{P}$, and we have replaced 1 by the length of the unit vector $\mathbf{u} = (\ell, m, n)$. Since $\mathscr{O}\mathscr{O}_1$ is parallel to $\mathbf{u}$ we obtain from (10.6), using a well known formula from vector calculus,

$$|\mathscr{Q}\mathscr{R}_2| = |\mathscr{Q}\mathscr{O}_2| - \frac{(x, y, 0) \cdot (\ell, m, n)}{M} = |\mathscr{Q}\mathscr{O}_2| - (\ell x + my)/M$$

This last result allows us to rewrite (10.2), using (10.1) and (4.5),

$$\varphi(x, y) = \iint_{-\infty}^{+\infty} \Psi(u, v) e^{i(2\pi/\lambda)|\mathcal{Q}\mathcal{O}_2|} e^{-i(2\pi/\lambda)[\ell x + my]/M} \, du \, dv$$

(10.7)

$$= \iint_{-\infty}^{+\infty} e^{i(2\pi/\lambda)[|\mathcal{O}\mathcal{O}_1\mathcal{Q}| + |\mathcal{Q}\mathcal{O}_2|]} \hat{A}(u, v) e^{-i2\pi[u(x/M) + v(y/M)]} \, du \, dv$$

The phase factor $e^{i(2\pi/\lambda)[|\mathcal{O}\mathcal{O}_1\mathcal{Q}| + |\mathcal{Q}\mathcal{O}_2|]}$ is a *constant, provided* the object plane and the image plane are *conjugate planes.*[6] In that case, as depicted in the classic imaging diagram shown in Figure 7.26, all the rays from $\mathcal{O}$, passing through various points $\mathcal{Q}$ in the focal plane, converge on a single point $\mathcal{O}_2$. Therefore, invoking Hamilton's form of Fermat's principle as we did in §4, we conclude that the wave fronts along those rays converge on $\mathcal{O}_2$ *in phase.* In particular, $e^{i(2\pi/\lambda)[|\mathcal{O}\mathcal{O}_1\mathcal{Q}| + |\mathcal{Q}\mathcal{O}_2|]}$ is a *constant* for all points $\mathcal{Q}$, equal to $e^{i(2\pi/\lambda)(d+D)}$ (taking $\mathcal{Q}$ on the optic axis). Thus, denoting this constant by e^{ic} for convenience, Eq. (10.7) becomes by Fourier inversion

$$\varphi(x, y) = e^{ic} \iint_{-\infty}^{+\infty} \hat{A}(u, v) e^{-i2\pi[u(x/M) + v(y/M)]} \, du \, dv$$

(10.8)

$$= e^{ic} A\left(-\frac{x}{M}, -\frac{y}{M}\right)$$

Equation (10.8) *expresses the well known fact that the image is an inverted copy of the object* (represented by its amplitude function A) *magnified by the factor* $M > 0$. (If $0 < M < 1$ then we might say *reduced* by the factor M.) If we observe φ by photographic film or by a viewing screen, then we record $|\varphi|^2 = |A(-x/M, -y/M)|^2$.

The key element of the discussion above was the Abbe sine condition (10.5), which is *much less restrictive* than the *small angle condition* $\alpha = M\bar{\alpha}$ of Gaussian optics (paraxial approximation).[7] Note also that our derivation reveals that imaging results from two diffraction (Fourier transform) processes. The second diffraction was treated by endowing the focal plane with *spatial frequency* coordinates (u and v) rather than spatial coordinates.

Not all optical systems obey the Abbe sine condition; high quality microscopes do but ordinary lenses do not. It is shown in optics texts [e.g., Goodman (1968) or Lipson and Lipson (1981)] that the upper limit to the angular field of view is provided by Abbe's sine condition; the lower limit is not really zero but rather the small angle condition mentioned above.

Until now we have pretended that the lens captures all the light from the object plane. We will now consider what happens when the lens is of finite size. As shown in Figure 7.4, we must now modify the transform $\hat{A}$ by allowing for missing spatial frequencies. We replace $\hat{A}$ in (10.8) by $\hat{A}P$ where P is a function for which $P(u, v) = 0$ when u or v is large enough.

6. In geometrical optics, this occurs when the *lens equation* $(1/d) + (1/D) = 1/f$ holds.

7. For this case, M is found to be D/d.

Then, by the convolution theorem

$$\varphi(x, y) = e^{ic} \iint_{-\infty}^{+\infty} \hat{A}(u, v) P(u, v) e^{-i2\pi[u(x/M) + v(y/M)]} \, du \, dv$$

(10.9)

$$= e^{ic} (A * \hat{P})\left(-\frac{x}{M}, -\frac{y}{M}\right)$$

Formula (10.9) says that the image is the magnified and inverted image of the convolution $A * \hat{P}$. The function P is called a *pupil function.* A typical example is

(10.10)

$$P(u, v) = \begin{cases} 1 & \text{if } (u^2 + v^2)^{1/2} < R \\ 0 & \text{if } (u^2 + v^2)^{1/2} > R \end{cases}$$

which corresponds to a spherical lens (well corrected for aberrations). In Figure 7.28 we show how this pupil function and its transform are related to the imaging of an object. In this example, the sharp cutoff (discontinuity) of P in the higher spatial frequencies results in the image $A * \hat{P}$ exhibiting a Gibb's phenomenon called *ringing.*

In many situations, such as natural light illumination, the object screen is not illuminated coherently. We do not have space to discuss the case of incoherent illumination. We shall only briefly describe the principal results. In this case the different phases in the illuminating wave combine, when

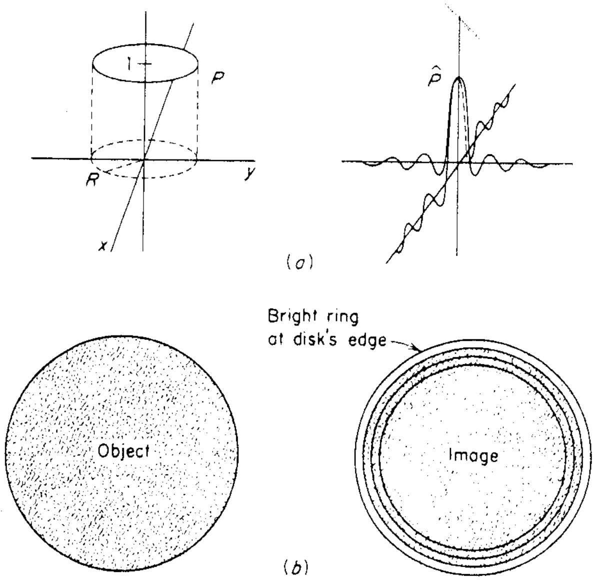

Figure 7.28 Ringing under coherent illumination. The bright ring on the image disk is a type of Gibb's phenomenon (for transforms). (*a*) A pupil function P and its transform $\hat{P}$. (*b*) Imaging of a disk. [See also Figures 6-12 and 6-13 in Goodman (1968).]

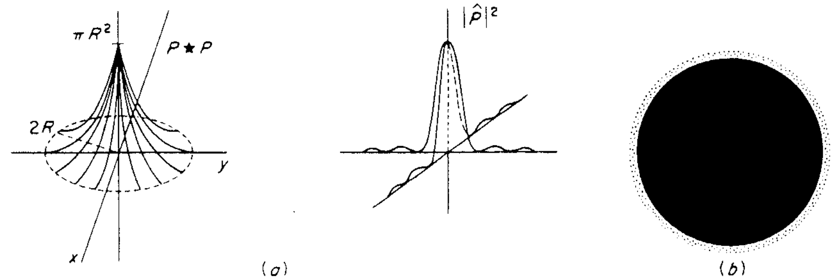

Figure 7.29 Loss of ringing, but blurring of image, under incoherent illumination. (*a*) Graphs of $P \star P$ and $|\hat{P}|^2$. Same P as in Figure 7.28. (*b*) Image of a black disk. [See also Figures 6-12 and 6-13 in Goodman (1968)].

focused onto the image plane, to yield only an *average* (over time) *intensity*. Formula (10.9) is replaced by

(10.11) $$|\varphi(x, y)|^2 = |A|^2 * |\hat{P}|^2\left(-\frac{x}{M}, -\frac{y}{M}\right)$$

Note that $|\hat{P}|^2$ is the transform of $P \star P$, the autocorrelation of the pupil function P. The details of deriving (10.11) are given in Iizuka (1985), §10.3. In Figure 7.29 we show that the ringing observed in coherent illumination is decreased to a blurring under incoherent illumination.

For further discussion of imaging, see Chapter 7 of Goodman (1968), Chapter 11 of Iizuka (1985), and Chapter 9 of Lipson and Lipson (1981).

Exercises

(10.12) Find $\hat{P}$ when $P(u, v) = \Pi(u/a)\Pi(v/b)$. Is there ringing, as shown in Figure 7.28, for this pupil function?

(10.13) Justify the graphs made of the pupil function P, its autocorrelation $P \star P$, and their transforms, shown in Figures 7.28 and 7.29.

(10.14) For what objects would rings (haloes, fringes) appear in the images, even under incoherent illumination, using the lens system described in Figure 7.29.

(10.15) Justify, using Fourier analysis, the following well known principle of optics: *The larger the lens opening (aperture) the better the image.*

(10.16) Show that (10.9) can be expressed in the form (ignoring the constant e^{ic})

$$(*)\quad \varphi(x, y) = h * \varphi_g(x, y) = \iint_{-\infty}^{+\infty} h(x - r, y - s)\varphi_g(r, s)\, dr\, ds$$

where

$$h(r, s) = \frac{1}{M}\hat{P}\left(-\frac{r}{M}, -\frac{s}{M}\right) \qquad \varphi_g(r, s) = A\left(-\frac{r}{M}, -\frac{s}{M}\right)$$

(φ_g stands for the image predicted by geometrical optics).

(10.17) Suppose that a sequence of m lenses is arranged along a single optic axis in such a way that the image plane of each lens coincides with the object plane of the next lens in the sequence. Justify the following optical principle: *The image quality from a system of lenses is limited by the smallest lens opening (aperture) in the system.*

(10.18) Show that, using coherent illumination and a circular lens, the smallest resolvable spatial detail in an object is approximately $1.22(\lambda d/a)$, where λ is the wavelength of the illumination, a is the radius of the circular lens aperture, and d is the distance from the object to the lens. [*Hint*: Use (4.8), (10.9), (10.10), and $M = D/d$.]

Part C. Signal Processing

§11. A Brief Introduction to Sampling Theory

The basic idea of sampling theory is the reconstruction of a function from an isolated collection, usually a periodic array, of data points. Sampling theory has major applications in several areas such as communications (telephone signal and optical processing), radio astronomy, and sound reproduction (digital recording).

Let's begin with a typical one-dimensional sampling theorem. A function g defined over $\mathbb{R}$ is said to be *limited* if for some positive constant c we have $g(x) = 0$ when $|x| \geq c$. The following theorem has been proved by several people working in different areas. It is called the sampling theorem by Nyquist, and by Shannon, and it is called the cardinal theorem of interpolation theory by Whittaker.

(11.1) Theorem. Suppose that f is continuous and absolutely integrable over $\mathbb{R}$ and $\hat{f}$ is limited. Then

$$f(x) = \sum_{n=-\infty}^{+\infty} f\left(\frac{n}{2c}\right) \operatorname{sinc}(2cx - n)$$

for all x values, provided $\hat{f}(u) = 0$ for $|u| \geq c$.

Proof. Because $\hat{f}(u) = 0$ for $|u| \geq c$, Fourier inversion yields

(11.2) $$f(x) = \int_{-c}^{c} \hat{f}(u)e^{i2\pi ux}\, du$$